Northumbria Research Link

Northumbria University NEWCASTLE

UniversityLibrary

An improved lumped parameter method for building thermal modelling

C. P. Underwood

Faculty of Engineering and Environment, University of Northumbria, UK

Abstract

In this work an improved method for the simplified modelling of the thermal response of building elements has been developed based on a 5-parameter second-order lumped parameter model. Previous methods generate the parameters of these models either analytically or by using single objective function optimisation with respect to a reference model. The analytical methods can be complex and inflexible and the single objective function method lacks generality. In this work, a multiple objective function optimisation method is used with a reference model. Error functions are defined at both internal and external surfaces of the construction element whose model is to be fitted and the resistance and capacitance distributions are adjusted until the error functions reach a minimum. Parametric results for a wide range (45) of construction element types have been presented. Tests have been carried out using a range of both random and periodic excitations in weather and internal heat flux variables resulting in a comparison between the simplified model and the reference model. Results show that the simplified model provides an excellent approximation to the reference model whilst also providing a reduction in computational cost of at least 30%.

Corresponding author: Tel +44-191-227-3533 Email: chris.underwood@northumbria.ac.uk

List of symbols

A	Area (m^2)
C	Thermal capacity per unit area ($Jm^{-2}K^{-1}$)
c	Specific heat capacity ($Jkg^{-1}K^{-1}$)
F	Fourier number
f	Thermal resistance rationing factor
g	Thermal capacity rationing factor
h	Surface convection coefficient ($Wm^{-2}K^{-1}$)
k	Thermal conductivity ($Wm^{-1}K^{-1}$)
L	Number of layers of material
m	Mass flow rate (kgs^{-1})
Q	Heat transfer (W)
R	Thermal resistance (m^2KW^{-1})
T	Temperature (^oC, K)
T'	Sol-air temperature (external), rad-air temperature (internal) (^oC)
t	Time (s)
W	Weighting factor
x	Distance (m)

Greek

α	Thermal diffusivity ($m^2 s^{-1} = k / \rho c$)
Δt	Time step increment (s)
Δx	Spatial increment (m)
ε	Root-mean-square error
ρ	Density ($kg m^{-3}$)
ΣC	Total element thermal capacity per unit area ($J m^{-2} K^{-1}$)
ΣR	Total element thermal resistance ($m^2 K W^{-1}$)

Subscripts and superscripts

a	Air, material ref. 'a'
b	Material ref. 'b'
c	Convection
i	Layer node index
i	Internal (space)
m	Middle position
n	Time row index
o	Outside, exterior
r	Radiant, solar radiation
s	Surface
s	Surface index number
upper	Upper bound limit

1. Introduction

In 2002 Gouda *et al*. [1] developed a simplified method for the dynamic thermal modelling of single-layer and multi-layer construction elements. They used an optimisation algorithm to find the five required parameters of the simplified model by matching its dynamic response to a high-order reference model. The work was limited in three respects:

- A unit step response was used as the excitation variable for the simplified model parameter fitting whereas excitations in practice vary continuously.
- The results were based on excitations applied individually to both heat flux and temperature at one surface only using a single objective function search algorithm whereas in practice, both internal and external surfaces would be subject to simultaneous excitations of more than one variable.
- Only two sets of results were published making it difficult for other users to make use of the simplified model.

In this work an improved method is proposed for the extraction of the simplified model parameters based on a multiple objective function search algorithm (i.e. objective functions simultaneously applied to both inside and outside surfaces) and the use of a reference model consisting of a rigorous finite-difference method. Extensive sets of results are generated for a range of common construction elements and a sample of these elements are tested in the context of a simple room enclosure model which alternately uses the simplified model and the more rigorous reference model for its construction elements.

2. Review

The application of lumped parameter modelling methods to building dynamic thermal response is motivated by the desire to find simpler and, hence, computationally less 'expensive' methods for the analysis building thermal energy response. Approaches broadly fall into two categories:

- Lumped parameter construction element models from which whole room models may be constructed [1, 2, 3]
- Lumped parameter whole room models [4, 5, 6, 7, 8]

Though the differences between the two approaches are rather subtle (since models of individual constructions elements are almost always used as a basis for grouping or aggregating into whole room models), the treatment of individual elements usually provide greater detail in modelling information such as individual surface temperatures which can be important when dealing with radiant sources, etc.

Lorenz and Masy [2] were among the first to propose a simplified lumped parameter approach to building response modelling using a first-order model consisting of two resistances and one capacitor. Gouda *et al*. [1] demonstrated improved accuracy using a second-order model in which each construction element is described using three resistances and two capacitances. These approaches to modelling were often referred to as 'analogue circuit' models due to their connotation with electric circuits (i.e. see Figure 1 in Section 4). Fraisse *et al*. [3] also compared first- and second-order element models (the latter referred to as a '3r2c' model) and went further to propose a fourth-order '3r4c' model with aggregated resistances. Like Lorenz and Masy [2], they propose an analytical method for deriving the parameters of the model (essentially, the distribution of resistance and capacitance values throughout the 'circuit') whereas Gouda *et al.* [1] used an optimisation method to determine the parameters with reference to a rigorous reference model.

Crabb *et al.* [4], Tindale [5] and others [6, 7, 8] have applied the lumped parameter approach to the formulation of low-order whole room models by casting the capacitance parameter over the higher capacity elements of a room (external walls, solid floors, etc) and using algebraic heat balances for the lower capacity room elements (demountable partitions, etc). Tindale [5] attempted this using a second-order room model but found that it provided unacceptable results for rooms with very high thermal capacity (i.e. 'traditional' construction). He corrected this by introducing a third 'equivalent' room capacitance which required an inconvenient method for its parameterisation.

Though low-order whole room models offer very low computational demands and simplicity, there remain questions over the accuracy of these models particularly over long time horizons and they tend to provide less modelling information (i.e. individual and accurate element surface temperatures) essential in many lines of design enquiry. For this reason, it is argued that room models constructed from second-order (or higher) construction element descriptions provide greater accuracy and detail whilst retaining some of the key advantages

of simplicity and low computational demand and are, therefore, to be preferred other than for approximate and early feasibility simulation studies.

The key advantages of lumped parameter building modelling are those of simplicity, transparency and low computational demand. They are particularly suited to bespoke (i.e. research-based) building response modelling using either modular-graphical modelling tools such as Simulink [9] – see for example [10, 11, 12], or equation-based methods such as Modelica [13] or EES [14, 15].

3. Reference Conduction Model

A key requirement for accuracy in simplified lumped parameter building models is the correct distribution of the overall element resistance and capacitance to ensure that the element surface temperatures are accurately predicted. It is possible to attempt this analytically as has been done by Lorenz and Masy [2] and Fraisse [3] however these methods usually require complicated mathematical models and are often restricted to defined surface input excitations. In the present work, an optimisation procedure is designed to adjust the resistance and capacitance distributions so that the surface temperature of the simplified model matches that of a rigorous reference model.

The reference construction element model was created from the one-dimensional energy equation using a finite-difference scheme:

$$\frac{\partial T}{\partial t} = \alpha \frac{\partial^2 T}{\partial x^2} \tag{1}$$

A full description of the discretisation and solution procedure of this equation as adopted in the present work applied to multi-layer construction elements can be found in [16]. A summary of the main discretised equations is given in the following for reference. For the temperature distribution through the body of each layer of material the following is used where the superscript n refers to the current time row and $n+1$ to the next time row:

$$T_i^{n+1} = \frac{1}{2F+1}\left(T_i^n + FT_{i-1}^{n+1} + FT_{i+1}^{n+1}\right) \tag{2}$$

in which the Fourier number, F, can be shown to be:

$$F = \alpha \frac{\Delta t}{\Delta x^2} \tag{3}$$

At the interfaces between two differing layers of material the interface temperature is obtained from the following (expressed here as the interface centred at the ith discrete slice forming a junction between two layers of different material, 'a' and 'b'):

$$T_i^{n+1} = T_i^n - \frac{2\Delta t}{\rho_a c_a \Delta x_a + \rho_b c_b \Delta x_b} \left(k_a \frac{\left(T_i^{n+1} - T_{i-1}^{n+1}\right)}{\Delta x_a} - k_b \frac{\left(T_{i+1}^{n+1} - T_i^{n+1}\right)}{\Delta x_b} \right) \tag{4}$$

And at a surface boundary, the temperature of the first discrete slice of the first layer of material is given by the following (in this case for the first slice of material on the inside surface layer which is taken to form slice 1 and bounded by room air at T_i with a surface convection coefficient of h_i):

$$T_1^{n+1} = T_1^n - \left(\frac{\Delta t}{\rho c \Delta x}\right) \cdot \left(k \frac{\left(T_1^{n+1} - T_2^{n+1}\right)}{\Delta x} - h_i \frac{\left(T_i^{n+1} - T_1^{n+1}\right)}{1 + h_i \Delta x / 2k} \right) \tag{5}$$

Finally, the temperature at the inside surface (of zero heat capacity) will be:

$$T_s^{n+1} = \frac{T_1^{n+1} + T_i^{n+1}\left(h_i \Delta x / 2k\right)}{1 + h_i \Delta x / 2k} \tag{6}$$

(a similar equation can be written for the temperature of the exterior surface).

The reference model was solved using a fully implicit scheme adopting Gauss-Seidel iteration. The discretisation scheme adopted one node at the centre of each layer of material and thus, with the interface equations, $2L+1$ conduction equations needed to be solved iteratively at each time step (where L is the number of layers of material) plus the two surface temperature equations.

4. Second-order Lumped Parameter Model

A simplified second-order construction element model can be used as an approximation to the much more rigorous description of the previous section. Gouda et al. [1] compared both first-order and second-order simplifications and concluded that the latter was an improvement on the former in terms of accuracy whilst requiring little additional computational effort. Figure 1 illustrates the parameters and variables of the second-order model based generally on that of Gouda et al. [1].
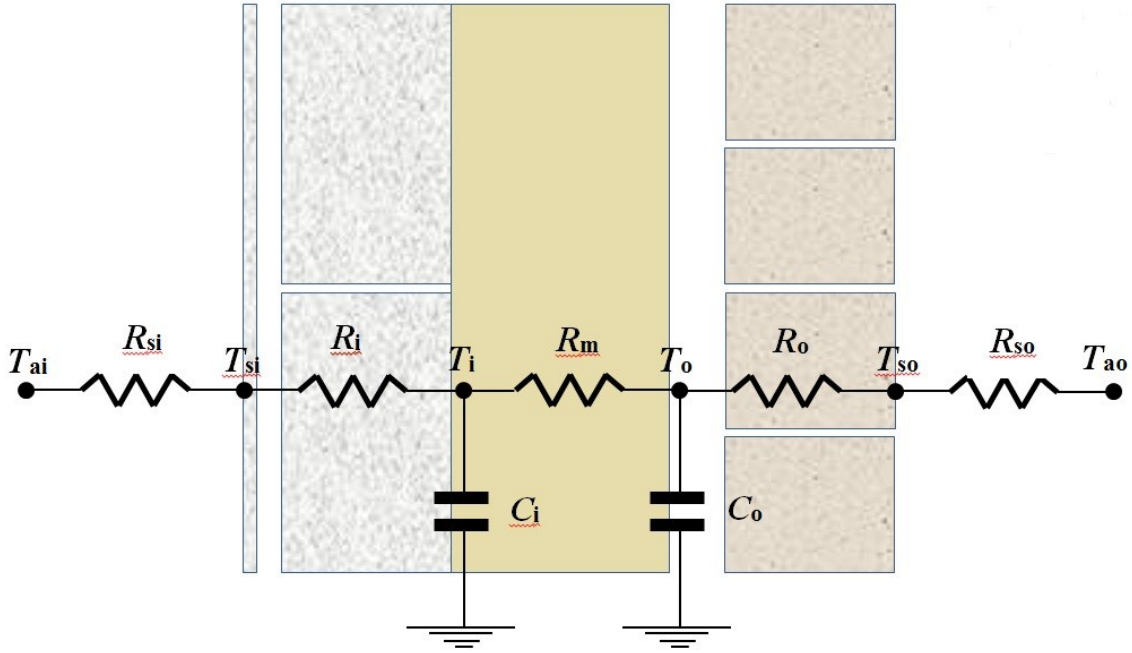
Figure 1 – Simplified 2nd-order construction element model

The overall thermal resistance between the inside and outside surfaces, ΣR (m^{2}KW^{-1}), can be easily calculated from material properties as can the overall thermal capacity per unit area, ΣC (Jm^{-2}K^{-1}). To generate the simplified model, the overall surface-to-surface resistance requires to be apportioned between the three series resistances, R_i, R_m and R_o, and the overall thermal capacity requires to be apportioned between the two capacitances, C_i and C_o such that:

$$R_i = f_i \Sigma R \tag{7}$$

$$R_o = f_o \Sigma R \tag{8}$$

$$R_m = \Sigma R - (R_i + R_o) \quad (f_m = 1 - (f_i + f_o)) \tag{9}$$

$$C_i = g_i \Sigma C \tag{10}$$

$$C_o = \Sigma C - C_i \quad (g_o = 1 - g_i) \tag{11}$$

Gouda *et al.* [1] referred to f_i, f_o, f_m, g_i and g_o as resistance and capacitance rationing factors. Thus a second-order model for a multi-layered construction element can be realised as follows.

$$g_i \Sigma C \frac{dT_i}{dt} = \frac{1}{f_i \Sigma R + R_{si}} (T_{ai} - T_i) - \frac{1}{(1 - f_i - f_o) \Sigma R} (T_i - T_o) \tag{12}$$

$$(1 - g_i) \Sigma C \frac{dT_o}{dt} = \frac{1}{(1 - f_i - f_o) \Sigma R} (T_i - T_o) - \frac{1}{f_o \Sigma R + R_{so}} (T_o - T_{ao}) \tag{13}$$

And the internal and external surface temperatures using this model will be:

$$T_{si} = \frac{R_i T_{ai} + R_{si} T_i}{R_i + R_{si}} \quad (14)$$

$$T_{so} = \frac{R_o T_{ao} + R_{so} T_o}{R_o + R_{so}} \quad (15)$$

This model can be completely parameterised by obtaining values for the three resistance and capacitance rations f_i, f_o and g_i.

In the original study, Gouda *et al.* [1] developed three alternative complete room models. The first used construction elements based on a high-order reference model. The second used the simplified second order model for the construction elements and the third used an existing first order model for comparative purposes. A single objective function search algorithm was applied to find values of the three rationing parameters which minimised the root-sum-square-error in the room air temperatures predicted by the second-order model and the reference model in response to a unit step change in either heat flux at the external surface (e.g. due to solar radiation) or external air temperature. The method and results given in this original study were limited in a number of respects:

- A whole room model was used to generate the parameter values making it difficult for the work to be replicated by other researchers and practitioners.
- A step response excitation for this application is unrealistic.
- The method would require to be repeatedly applied for different disturbance variables and is inapplicable when more than one excitation variable are simultaneously active.
- There was an insufficient number of results for alternative construction types making it difficult to utilise the model for a range of alternative applications.

The method and results reported in the following sections attempt to address these shortcomings in the following ways:

a) A multiple objective function search algorithm is used with simultaneous disturbances applied to both inside and outside surfaces of the reference and target models.
b) The proposed new method is applied at the construction element level by targeting surface (rather than room) temperatures thus making the method easier to replicate by other researchers and practitioners.
c) The method is tested at room level in relation to room temperature response to demonstrate robustness.
d) A periodic function is used to drive the excitation variables.
e) A large number of results are generated and reported for a range of alternative construction elements making the model easy for students, researchers and practitioners to apply without needing to carry out a parameter-fitting analysis.

5. Optimised Parameter Fitting Method

A function was created to implement the two models described in sections 4 and 5 for a defined single or multi-layer construction element. The internal and external air temperatures were varied sinusoidally with peak-to-peak amplitudes of 1K and a period of 24h consistent with a diurnal cycle. The internal and external surface temperatures predicted by eqns. (6) (reference model), and eqns. (14 & 15) (second-order model) were obtained and root-mean-square error values between the two sets of surface temperatures ($\varepsilon_{T_{\mathrm{si}}}, \varepsilon_{T_{\mathrm{so}}}$ for the internal and external surface errors respectively) were returned as a function of values of the three rationing parameters, $f_{\mathrm{i}}, f_{\mathrm{o}}$ and g_{i}. The followuing optimisation problem was then set up:

$$\min_{f_{\mathrm{i}}, f_{\mathrm{o}}, g_{\mathrm{i}}} \left(\varepsilon_{T_{\mathrm{si}}}, \varepsilon_{T_{\mathrm{so}}} \right) \text{ subject to:} \begin{cases} W\left(\varepsilon_{T_{\mathrm{si}}}\right), W\left(\varepsilon_{T_{\mathrm{so}}}\right) \leq Goal \\ \left[f_{\mathrm{i}}, f_{\mathrm{o}}, g_{\mathrm{i}} \right] \geq \left[0, 0, 0 \right] \\ \left[f_{\mathrm{i}}, f_{\mathrm{o}}, g_{\mathrm{i}} \right] \leq \left[f_{\text{i-upper}}, f_{\text{o-upper}}, g_{\text{i-upper}} \right] \end{cases} \tag{16}$$

An active-set optimisation algorithm was used with a single objective function derived from an importance weighting of the two fundamental objective functions, $\varepsilon_{T_{\mathrm{si}}}, \varepsilon_{T_{\mathrm{so}}}$. Unity weightings were applied to both of the root objective functions in the work reported here to signify that both internal and external surface temperature targets were equally important. (In practice, the Matlab function 'fgoalattain' was used for the above [17].)

6. Improved Second-order Lumped Parameter Model – Results

The optimisation algorithm was applied to a wide range of typical construction elements grouped into 4 categories:

- Internal partitions (14 examples)
- Floors (8 examples)
- Roofs (8 examples)
- External walls (15 examples)

The overall surface-to-surface resistances (including allowances for interstitial air gaps where relevant) and overall thermal capacities were calculated using material properties listed in CIBSE Guide, Book A [18].

Results for the various construction elements are given in the tables in Appendix A. The tables list the resistance rations (internal zone, middle and outer zone) and capacitance rations (internal zone and outer zone) so that the simplified lumped parameter construction element model described in Section 4 can be fully parameterised for any chosen element. As might be expected, for single layer elements or multi-layer elements with symmetrical layering, the

results show that $f_i = f_o$ and $g_i = g_o = 0.5$. For multi-layer elements with many layers (e.g. >4) the middle zone resistance tends to dominate.

7. Model Testing

In order to investigate the accuracy and robustness of the simplified model to building thermal response with a range of both periodic and random excitations several of the construction elements whose results are listed in Appendix A were formed into a simple (and somewhat arbitrary) room enclosure. The test room enclosure was assumed to have dimensions of 10m x 5m x 3m-high forming a corner of a building facing south and west with an exposed roof, internal floor and internal partitions forming the north and east edges. There were no windows defined. The CIBSE/Met Office test reference year for London Heathrow [19] was used to define the conditions at the room enclosure exterior and the enclosure was completed with the following internal air volume heat balance:

$$C_{ai} \frac{dT_{ai}}{dt} = Q_c + m_{vent} c_{ai} (T_{ao} - T_{ai}) + \sum_{s=1}^{s=5} A_s h_s (T_s - T_{ai}) \qquad (17)$$

In eqn. (17), Q_c is convective heat added directly to the room air and m_{vent} is an assumed continuous rate of flow of external ventilation air that enters the enclosure (with the same amount of air leaving). The enclosure air volume was assumed to be perfectly mixed at all times. The 5 internal surfaces referenced in eqn. (17) refer to the external wall (south), external wall (west), floor, ceiling and internal partitions. Eqn. (17) was solved separately based on surface temperatures predicted by the reference model and surface temperatures predicted by the simplified model. The internal enclosure elements (floor and partitions) were treated as adiabatic elements by imposing exactly the same conditions on the opposite sides as in the subject space. To deal with radiant heat fluxes, air temperatures in eqns. (6, 14 & 15) were replaced with sol-air temperatures at exterior surfaces and an equivalent surface rad-air temperature at interior surfaces (similar to that first proposed by Davies [20] however, for the present purpose, radiant interchange between room surfaces was not considered). The exterior sol-air and interior rad-air temperatures are given by the following for some interior surface s_i and exterior surface s_o:

$$T'_{ao,s_o} = T_{ao} + \frac{Q_{r,s_o}}{h_{s_o}} \qquad (18)$$

$$T'_{ai,s_i} = T_{ai} + \frac{Q_{r,s_i}}{h_{s_i}} \qquad (19)$$

Two separate tests were carried out:

- A moderately high thermal capacity test using external wall type 6 (Appendix A, Table A1.4), roof type 5 (Appendix A, Table A1.3), floor type 5 (Appendix A, Table A1.2) and partition type 9 (Appendix A, Table A1.1) giving an overall enclosure fabric thermal capacity of 48.9MJK^{-1}.

- A low thermal capacity test using external wall type 2 (Appendix A, Table A1.4), roof type 3 (Appendix A, Table A1.3), floor type 1 (Appendix A, Table A1.2) and partition type 1 (Appendix A, Table A1.1) giving an overall enclosure fabric thermal capacity of 6.8MJK^{-1}.

The tests consisted of one complete annual simulation in each case, using the weather file.

The global horizontal solar radiation in the weather file was first pre-processed into annual time-series surface irradiances relevant to the south- and west-facing walls and the horizontal roof surface using the clearness index model of Skartveith and Olseth [21]. A ground reflection factor of 0.2 was assumed and a surface absorption coefficient of 0.9 was used for all surfaces. The results were then used in eqn. (18) to determine time-series sol-air temperatures for each surface together with the corresponding external air temperature from the weather data.

m_{vent} was calculated by assuming a constant rate of ventilation equivalent to 0.5 of an air change per hour. An internal heat excitation rate of 1kW (20Wm^{-2} of floor area) was ramped in each day of the simulation between 07:00h and 10:00h and then ramped back down to zero between 18:00h and 21:00h after being held constant between these times. Half of this energy was allocated to convection (entering via the Q_c term in eqn. (17)) and the remaining half was uniformly added to each surface as radiation (entering via the rad-air temperatures of eqn. (19)).

Though the conditions defined above are somewhat arbitrary, they are considered sufficient to capture a wide range of the important variables that are likely to be of primary influence over the behaviour of a construction fabric dynamic thermal model.

Results of the two tests are presented in the following. They were obtained using an integration time step of 1 minute over one complete annual cycle. The reference model used a single central node for each layer of material such that each layer of material was completely defined by 3 nodes (one at the centre and two interface nodes). Thus $2L+1$ equations (where L is the number of material layers) required to be solved for the reference model whereas just 2 equations require to be solved for all instances of the simplified model (excluding surface equations in both cases).

Comparisons of the enclosure air temperature predicted by both models are given in figures 2 and 3. Figure 2 shows that the simplified model gives an excellent agreement with the reference model for a traditional high thermal capacity construction. Figure 3 shows that the agreement is adequate for a low thermal capacity construction though not as good as for high thermal capacity. This conclusion is also evident in the results of surface temperature comparison shown in Figure 4 (high thermal capacity) and Figure 5 (low thermal capacity). The surface temperature comparisons show a good level of agreement over a very wide range

of operating surface temperatures particularly the exterior surfaces of the external wall and roof where solar radiation is responsible for some high surface temperature behaviour.
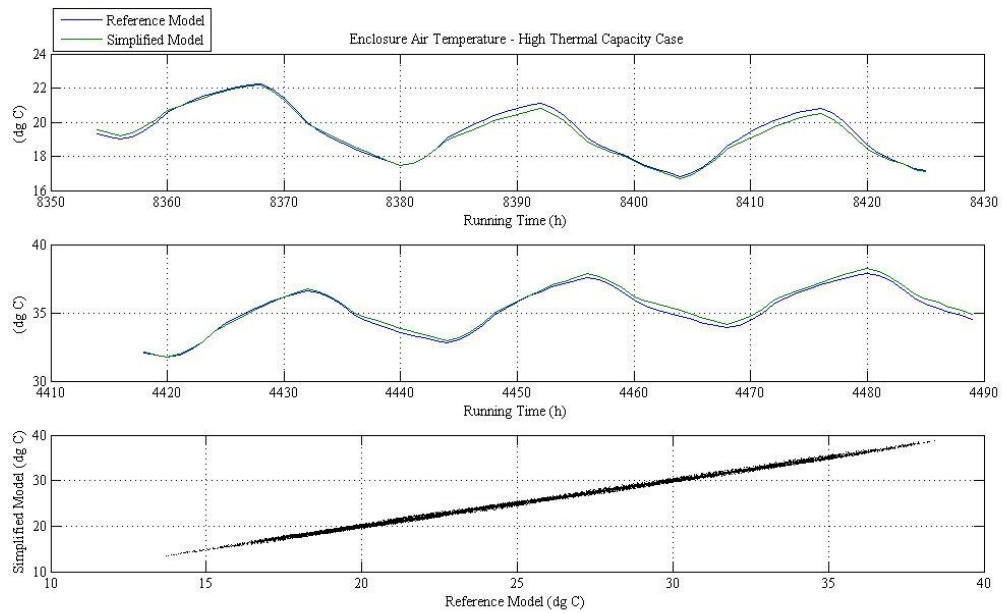
Figure 2 – Enclosure air temperature comparisons (high thermal capacity)
(Top: Three day sample, winter / Middle: Three day sample, summer / Bottom: All data)
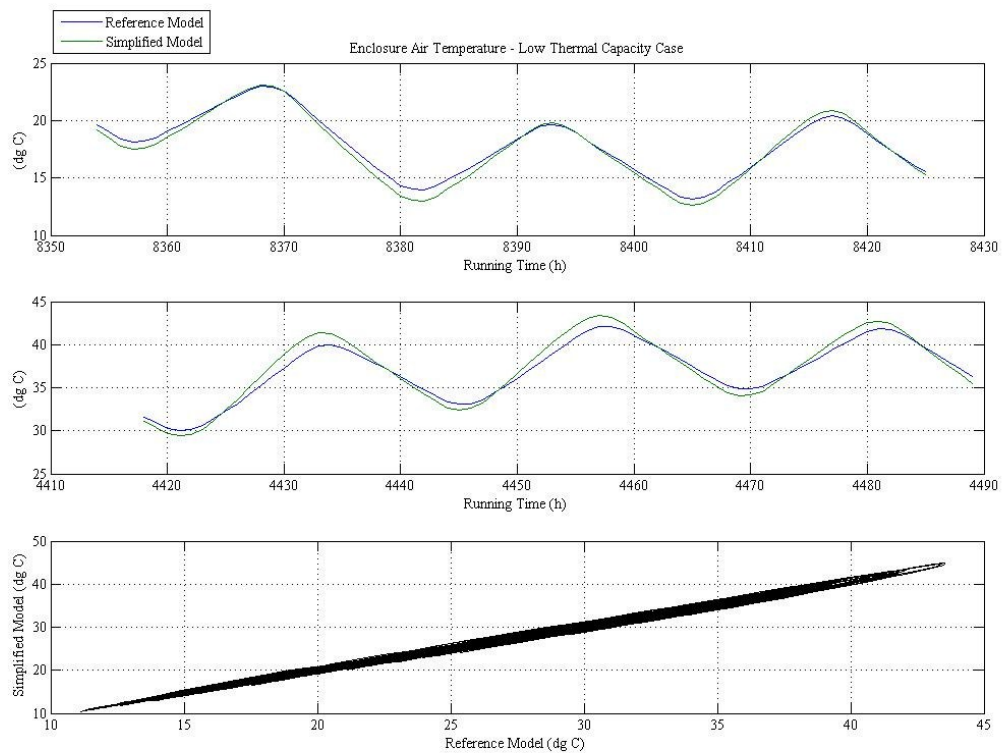
Figure 3 – Enclosure air temperature comparisons (low thermal capacity)
(Top: Three day sample, winter / Middle: Three day sample, summer / Bottom: All data)

Figure 4 – Fabric surface temperature agreements (high thermal capacity)

Figure 5 – Fabric surface temperature agreements (low thermal capacity)

The overall RMS error results are given in Table 1. The overall average RMS errors resulting from the two models over all surface temperatures and the internal air temperature are 0.30K (high thermal capacity) and 0.43K (low thermal capacity).

Table 1 – RMS errors in key variables between the reference and simplified models

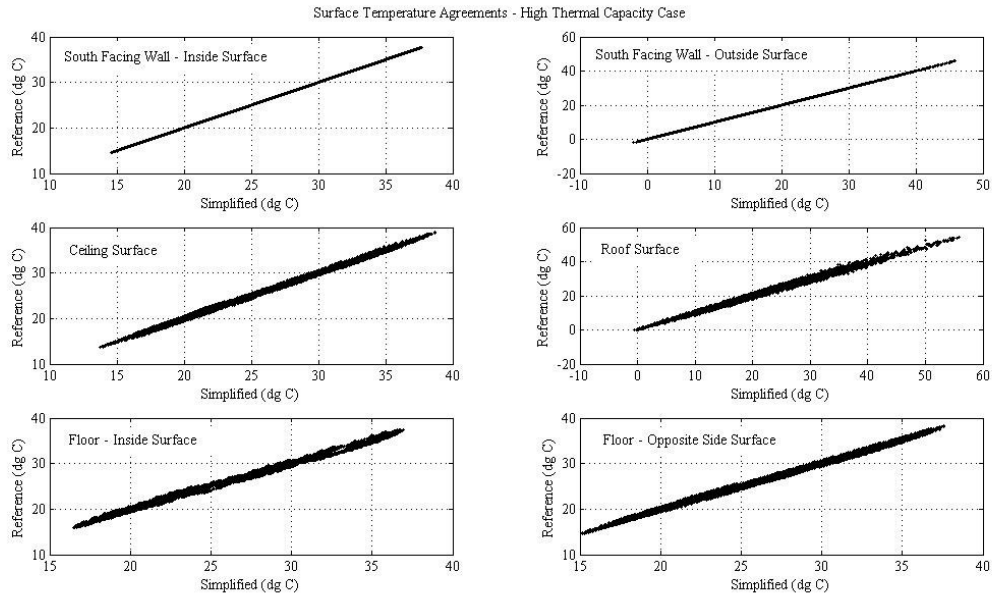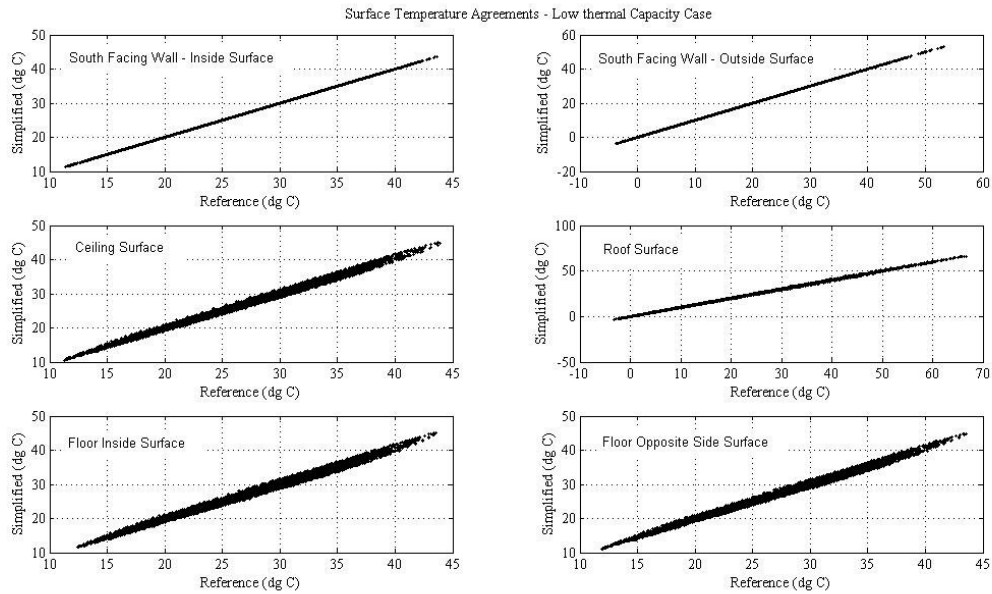| Variable	High thermal capacity test	Low thermal capacity test
Air temperature	0.24	0.50
External wall (south) inside surface temperature	0.25	0.43
External wall (south) outside surface temperature	0.18	0.11
External wall (west) inside surface temperature	0.25	0.43
External wall (west) outside surface temperature	0.18	0.11
Internal floor inside surface temperature	0.38	0.66
Internal floor opposite surface temperature	0.32	0.57
Ceiling surface temperature	0.29	0.53
Roof outside surface temperature	0.74	0.22
Partition inside surface temperature	0.22	0.59
Partition opposite surface temperature	0.22	0.59
Mean over all variables	0.30	0.43

The computational elapsed time using the reference model only was 9.1 minutes (high thermal capacity test case) and 9.8 minutes (low thermal capacity test case). When using the simplified model only, the computational elapsed time reduced to 6.5 minutes (both cases) – a reduction of around 30%.

Results were also generated using alternative integration time intervals of 5 minutes and 10 minutes (the default time step used in a number of commercially available energy simulation programs). The RMS errors did not change significantly at these wider time steps. To a certain extent this is to be expected since the conduction calculations are performed using an implicit calculation algorithm (though at very wide time steps the accuracy would be expected to begin to suffer). However the computation times reduced to an average of 2.6 minutes (reference model) and 1.3 minutes (simplified model) at an integration interval of 5 minutes and an average of 1.6 minutes (reference model) and 0.7 minutes (simplified model) at the higher integration time step.

8. Comparisons with Established Methods

The advantages of the simplified building element model developed in this work are those of simplicity, transparency and ease of implementation compared with established methods. Though not suited to rigorous detailed simulations of multi-zone buildings, the simplified

method is particularly suited to smaller (e.g. 1-3 zone) building response modelling using modular-graphical or equation-based modelling tools as are frequently used in building energy research or in bespoke building design practice. The model developed here has been fitted to a range of building element thermal responses generated using a detailed finite-difference numerical model. The finite-difference numerical method for conduction calculations is used in several established energy simulation tools including 'ApacheSim' which forms part of IES, the predominant energy simulation program used by practitioners in the UK [22], and 'ESP-r' which is a long-standing freeware-based energy simulation program used mainly by researchers [23]. However, arguably the dominant method of performing these calculations is through the use of conduction transfer functions which are used in many of the early simulation programs such as 'BLAST' and 'DOE-2' and, more recently, a very widely used program which was formed out of these two called 'EnergyPlus' [24].

In order to explore the performance of the simplified model developed in this work with the use of the conduction transfer function (CTF) method, a further simple test was conducted. An example cooling load transient performed using CTFs on a 5-layer external wall construction with defined internal and external surface temperatures was described by Spitler [25]. Details of the data used, and the transient cooling load results obtained, are given in Appendix 2. The optimisation method described in Section 5 was applied to Spitler's example construction using the finite-difference reference model described in Section 3 and the following results were obtained for the simplified lumped parameter model:

$$f_i = 0.100 \; ; f_m = 0.866 \; ; f_o = 0.034 \; ; g_i = 0.360 \; ; g_o = 0.640$$

The simplified model was then applied using the above parameter settings and Spitler's surface temperatures [25] as listed in Appendix 2. The results of internal cooling load surface heat fluxes are compared in Figure 6. The root-mean-square error between Spitler's results [25] and the simplified model was found to be 0.0286 (i.e. < 3%). Thus the simplified model fitted using a finite-difference reference model appears to offer a very good approximation to the traditional CTF conduction modelling method.
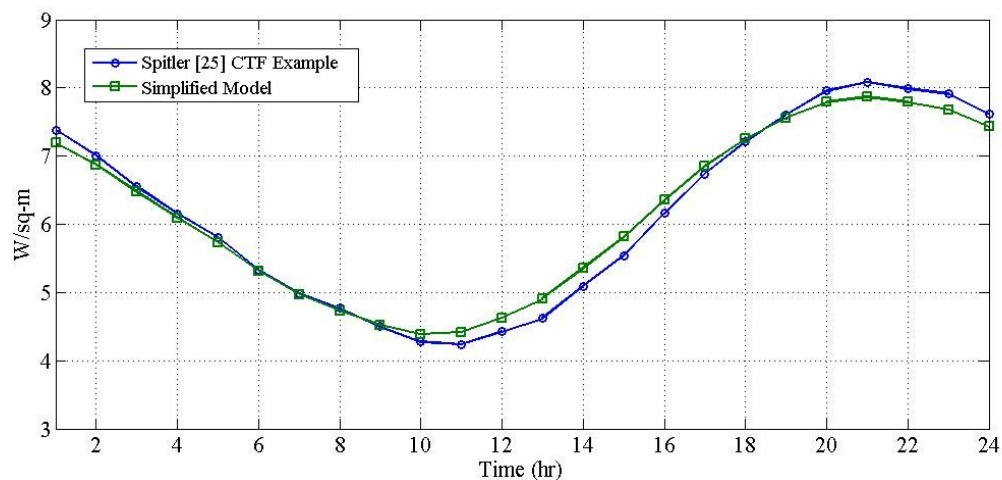

Figure 6 – Simplified and CTF model response comparison of surface heat flux transient

9. Conclusions

In this work an improved method for the simplified modelling of the thermal response of building elements has been developed. The simplified model is based on a 5-parameter second-order method with 3 series resistances and 2 capacitances. A rigorous reference model has been developed based on an implicit finite-difference solution of the governing energy equation. Objective functions consisting of root-mean-square errors in both internal and external surface temperatures predicted by the simplified model and reference model have been defined. The surfaces have been excited using sinusoidally-varying air temperatures at both surfaces and the parameters of the simplified model were adjusted until the surface temperature errors declined to a minimum. Resistance and capacitance modelling parameter results for a wide range (45) of construction element types have been presented. Tests have been carried out using a range of both random and periodic excitations in weather and internal heat flux variables enabling a comparison to be made between the simplified model and the reference model. The tests were conducted on a sample of the generated construction element types for both high thermal capacity and low thermal capacity examples. Results of the tests show that the simplified model provides an excellent approximation to the reference model especially when used for the simulation of the thermal response of a room enclosure with 'traditional' construction types of relatively high thermal capacity whilst also providing a reduction in computational cost of at least 30%. The results further show a good agreement with the conduction transfer function modelling method which is used in many of the established energy simulation programs available today. The simplified model has the advantage of requiring the solution of just 2 equations as opposed to a minimum of 3 (for a single-layer element) and as many as 11 equations (for a 5-layer element) in the case of the reference model.

The model is most suitable for use by students and researchers for developing bespoke building models using either modular-graphical modelling tools or equation-based modelling methods. Further work is merited to incorporate moisture mass transfer effects to give an alternative simultaneous model of heat and mass transfer in construction elements.

References

[1] Gouda MM, Danaher S, Underwood CP. Building thermal model reduction using nonlinear constrained optimization. Building and Environment 2002; 37:1255-65.

[2] Lorenz F, Masy G. Methode d'evaluation de l'economie d'energie apportee par l'intermittence de chauffage dans les batiments. Traitement par differences finies d'un model a deux constantes de temps. Report no. GM820130-01. Faculte des Sciences Appliquees, University de Liege, Liege, Belgium; 1982 (in French).

[3] Fraisse G, Viardot C, Lafabrie O, Achard G. Development of a simplified and accurate building model based on electrical analogy. Energy and Buildings 2002; 34: 1017-31.

[4] Crabb JA, Murdoch N, Penman JM. A simplified thermal response model. Building Services Engineering Research and Technology 1987; 8: 13-9.

[5] Tindale A. Third-order lumped-parameter simulation method. Building Services Engineering Research and Technology 1993; 14(3): 87-97.

[6] Nielsen TR. Simple tool to evaluate energy demand and indoor environment in the early design stages. Solar Energy 2005; 78: 73-83.

[7] Kämpf JH, Robinson D. A simplified thermal model to support analysis of urban resource flows. Energy and Buildings 2007; 39: 445-53.

[8] Antonopoulos KA, Koronaki EP. On the dynamic thermal behaviour of indoor spaces. Applied Thermal Engineering 2001; 21: 929-40.

[9] SIMULINK Simulation and model-based design. Available at: http://www.mathworks.co.uk/products/simulink/ [Accessed: 12 July 2013.]

[10] Henze GP, Neumann C. Building Performance Simulation for Design and Operation (eds. Hensen JLM, Lamberts R). London: Spon Press; 2011, Chapter 14, p. 436-40.

[11] SIMBAD building and HVAC modelling toolbox for Matlab/Simulink. Available at: http://www.simbad-cstb.fr/ [Accessed: 12 July 2013.]

[12] Kalagasidis AS *et al*. The International Building Physics Toolbox in Simulink. Energy and Buildings 2007; 39: 665-74.

[13] Modelica – A unified object-oriented language for physical systems. Available at: http://www.modelica.org/documents/ModelicaSpec32.pdf [Accessed: 12 July 2013.]

[14] F_Chart software: EES – Engineering Equation Solver. Available at: http://www.fchart.com/ees [Accessed: 12 July 2013.]

[15] Bertagnolio S, Lebrun J. Simulation of a building and its HVAC system with an equation solver: Application to benchmarking. Building Simulation 2008; 1: 234-50.

[16] Underwood CP, Yik FWH. Modelling Methods for Energy in Buildings. Oxford: Wiley-Blackwell; 2004, p. 47-56.

[17] Mathworks documentation centre – *fgoalattain*. Available at: http://www.mathworks.co.uk/help/optim/ug/fgoalattain.html [Accessed: 5 July 2013.]

[18] CIBSE Guide Book A Section A3 – Thermal Properties of Building Structures (5th edition). London: Chartered Institution of Building Services Engineers; 1988, Table A3.15, pA3-22.

[19] Weather data and climate change information. London: Chartered Institution of Building Services Engineers. Available at: http://www.cibse.org/index.cfm?go=page.view&item=1300 [Accessed: 7 July 2013.]

[20] Davies MG. Rad-air temperature: The global temperature in an enclosure. Building Services Engineering Research & Technology 1989; 10(3): 89-104.

[21] Skartveit A, Olseth JA. A model for the diffuse fraction of hourly global radiation. Solar Energy 1987; 38(4): 271-4.

[22] ApacheSim Calculation Methods. Glasgow: Integrated Environmental Solutions Ltd. Available at:
http://www.iesve.com/downloads/help/Thermal/Reference/ApacheSimCalculationMethods.pdf [Accessed: 16 January 2014.]

[23] Clarke JA. Energy Simulation in Building Design. Oxford: Butterworth Heinemann; 2001, Appendix G, p. 355-6.

[24] EnergyPlus Energy Simulation Software – EnergyPlus Documentation. USA Department of Energy. Available at:
http://apps1.eere.energy.gov/buildings/energyplus/energyplus_documentation.cfm [Accessed: 16 January 2014.]

[25] Spitler JD. Building Performance Simulation for Design and Operation (eds. Hensen JLM, Lamberts R). London: Spon Press; 2011, Chapter 5, p. 94-5.

APPENDIX 1 – Results of fitting to a range of common construction element types

The parameter fitting results for a wide range of construction element types are given in tables A1.1 – A1.4 based on the following notation:

Example: PB13 – 13mm thick plasterboard

Symbols used:

ACS	Aerated concrete slab
AS	Asphalt
B	Brick
CL	Concrete, light
CH	Concrete, high density
CBL	Concrete block, light
CBH	Concrete block, high density
MC	Metallic cladding
MFS	Mineral fibre slab
P	Plaster, light
PB	Plasterboard
SC	Stone chippings
SCR	Screed
SO	Soil, compacted
SW	Softwood
RT	Roof tile
WS	Woodwool slab

Note that the overall resistances (ΣR in the following tables) are surface-to-surface (i.e. excluding surface resistances). Other symbols are defined in the List of Symbols. All resistances and thermal capacities are calculated based on data contained in the CIBSE Guide, Book A [18].

TABLE A1.1 Results for partitions

PARTITIONS (from inside to outside)	ΣR (m^{2}KW^{-1})	ΣC (JK^{-1})	f_i	f_m	f_o	g_i	g_o
1. PB13/Airgap/PB13	0.3425	20869	0.063	0.874	0.063	0.500	0.500
2. PB13/MFS75/PB13	2.3054	22998	0.012	0.976	0.012	0.500	0.500
3. PB13/MFS100/PB13	3.0196	23748	0.010	0.980	0.010	0.500	0.500
4. B105	0.1694	142800	0.500	0	0.500	0.500	0.500
5. B220	0.3548	299200	0.308	0.384	0.308	0.500	0.500
6. PB13/Airgap/B105/Airgap/PB13	0.6919	163572	0.316	0.368	0.316	0.500	0.500
7. PB13/Airgap/B220/Airgap/PB13	0.8773	319972	0.305	0.390	0.305	0.500	0.500
8. P13/B105	0.2506	150600	0.498	0.307	0.195	0.440	0.560
9. P13/B105/P13	0.3319	158400	0.250	0.500	0.250	0.500	0.500
10. P13/B220	0.4361	307000	0.269	0.499	0.232	0.368	0.632
11. P13/B220/P13	0.5173	314800	0.242	0.516	0.242	0.500	0.500
12. CBL200	1.0526	120000	0.300	0.400	0.300	0.500	0.500
13. P13/CBL200	1.1339	127800	0.119	0.622	0.259	0.390	0.610
14. P13/CBL200/P13	1.2151	135600	0.121	0.758	0.121	0.500	0.500

TABLE A1.2 Results for floor

FLOORS (from inside to outside)	ΣR (m^{2}KW^{-1})	ΣC (JK^{-1})	f_i	f_m	f_o	g_i	g_o
1. SW20/Airgap/PB13	0.4241	26155	0.067	0.793	0.140	0.500	0.500
2. SW20/CL100/Airgap/PB13	0.6873	146155	0.242	0.470	0.288	0.622	0.378
3. SW20/CL200/Airgap/PB13	0.9504	266155	0.200	0.511	0.289	0.547	0.453
4. SCR25/CH100/Airgap/PB13	0.4137	212155	0.184	0.351	0.465	0.662	0.338
5. SCR40/CH100/Airgap/PB13	0.4502	227275	0.193	0.345	0.462	0.650	0.350
6. SCR40/CH200/Airgap/PB13	0.5217	403675	0.205	0.276	0.519	0.561	0.439
7. SCR40/CL100/MSF50/SO500	2.2438	961820	0.044	0.900	0.056	0.176	0.824
8. SCR40/MFS50/CH200/SO500	2.1235	1194620	0.200	0.706	0.094	0.471	0.529

TABLE A1.3 Results for roofs

ROOFS (from inside to outside)	ΣR (m^{2}KW^{-1})	ΣC (JK^{-1})	f_i	f_m	f_o	g_i	g_o
1. PB13/Airgap/MFS250/RT10	7.4160	33436	0.007	0.988	0.005	0.444	0.556
2. PB13/Airgap/MFS300/SW20/RT10	8.9874	50536	0.010	0.986	0.004	0.274	0.726
3. PB13/Airgap/MFS250/WS50/AS10	7.9041	60236	0.012	0.980	0.008	0.265	0.735
4. PB13/MFS250/Airgap/ACS100/AS10	8.0291	77236	0.015	0.974	0.011	0.236	0.764
5. PB13/MFS250/Airgap/CH200/AS10/SC10	7.5574	406036	0.023	0.969	0.008	0.065	0.935
6. PB13/MFS300/SW20/AS10	8.8155	831974	0.009	0.988	0.003	0.297	0.703
7. SW20/Airgap/MSF300/MC05	8.8944	43682	0.010	0.990	0	0.419	0.581
8. PB13/MFS300/Airgap/MC05	8.8328	19736	0.021	0.979	0	0.330	0.670

TABLE A1.4 Results for external walls

EXTERNAL WALLS (from inside to outside)	ΣR (m^{2}KW^{-1})	ΣC (JK^{-1})	f_i	f_m	f_o	g_i	g_o
1. PB13/Airgap/MFS200/SW20	6.1184	32034	0.009	0.979	0.012	0.474	0.526
2. PB13/Airgap/MFS300/SW20	8.9755	35034	0.008	0.982	0.010	0.470	0.530
3. PB13/Airgap/MFS200/MC05	5.9756	35154	0.030	0.970	0	0.363	0.637
4. PB13/Airgap/MFS300/MC05	8.8328	38154	0.007	0.993	0	0.354	0.646
5. PB13/Airgap/CBL105/MFS200/B105	6.6532	222186	0.036	0.955	0.009	0.237	0.763
6. PB13/Airgap/CBL105/MFS300/B105	9.5103	225186	0.026	0.967	0.007	0.234	0.766
7. PB13/Airgap/CBH105/MFS200/B105	6.1650	400686	0.042	0.949	0.009	0.515	0.485
8. PB13/Airgap/CBH200/MFS200/B105	6.2232	619186	0.046	0.945	0.009	0.662	0.338
9. PB13/Airgap/CBH105/MFS300/B105	9.0221	403686	0.029	0.965	0.006	0.516	0.484
10. PB13/Airgap/CBH200/MFS300/B105	9.0804	842602	0.032	0.962	0.006	0.662	0.338
11. CBL105/Airgap/MFS200/B105	6.5719	211860	0.034	0.958	0.008	0.273	0.727
12. CBH200/Airgap/MFS300/B105	8.9991	611860	0.005	0.989	0.006	0.722	0.278
13. CBL105/Airgap/MFS300/MC05	9.3042	90780	0.024	0.975	0.001	0.659	0.341
14. CBH105/Airgap/MFS300/MC05	8.8159	269280	0.003	0.997	0	0.912	0.088
15. CBH200/Airgap/MFS300/MC05	8.8742	487780	0.005	0.994	0.001	0.919	0.081

APPENDIX 2 – Spitler's [25] conduction transfer function example data

TABLE A2.1   Example external wall construction details [25]

MATERIAL (from inside to outside)	Thickness (mm)	Density (kgm^{-3})	Conductivity (Wm^{-1}K^{-1})	Specific Heat Capacity (Jkg^{-1}K^{-1})
1. Plasterboard	13	720	0.16	840
2. Solid concrete block	100	2096	1.63	920
3. Insulation	50	91	0.04	840
4. Air gap	20	1	0.11	1005
5. Facing brick	100	1920	0.87	800

TABLE A2.2   CTF coefficients for the construction described in Table A2.1 [25]

j	X_j	Y_j	Z_j	Φ_j
0	2.171573×10^1	3.375092×10^{-5}	1.033658×10^1	-
1	-4.514066×10^1	5.617864×10^{-3}	-1.794393×10^1	1.463783×10^0
2	2.844604×10^1	2.266381×10^{-2}	8.642595×10^0	-5.568298×10^{-1}
3	-5.162262×10^0	1.133217×10^{-2}	-1.021217×10^0	2.488959×10^{-2}
4	1.826630×10^{-1}	8.227039×10^{-4}	2.664688×10^{-2}	-2.266001×10^{-4}
5	-1.023128×10^{-3}	8.775257×10^{-6}	-1.882663×10^{-4}	-

TABLE A2.3   Boundary conditions and results [25]

Time (h)	Inside Surface temperature (^{o}C)	External surface temperature (^{o}C)	Inside surface heat flux (Wm^{-2})
1	26.42	22.09	7.34
2	25.44	22.08	6.97
3	24.67	22.07	6.58
4	24.08	22.05	6.18
5	23.89	22.02	5.78
6	24.28	22.00	5.39
7	25.25	21.97	5.02
8	27.00	21.93	4.71
9	29.53	21.90	4.46
10	32.44	21.88	4.31
11	35.75	21.86	4.28
12	38.86	21.84	4.40
13	41.19	21.84	4.67
14	42.75	21.84	5.07
15	43.33	21.86	5.57
16	42.75	21.88	6.13
17	41.39	21.91	6.70
18	39.25	21.95	7.22
19	36.72	21.99	7.64
20	34.19	22.02	7.92
21	32.06	22.05	8.06
22	30.11	22.08	8.05
23	28.56	22.09	7.90
24	27.39	22.10	7.66